

The utility of forest attribute maps for automated Avalanche Terrain Exposure Scale (ATES) modelling

Johannes Schumacher*¹, Håvard Toft Larsen^{2,3}, J. Paul McLean¹, Marius Hauglin¹, Rasmus Astrup¹, Johannes Breidenbach*¹

¹ Norwegian Institute of Bioeconomy Research (NIBIO), Ås, Norway

² Norwegian Water Resources and Energy Directorate (NVE), Oslo, Norway

³ UiT The Arctic University of Norway, Center for Avalanche Research and Education, Tromsø, Norway

* Correspondence: Johannes.Schumacher@nibio.no, Johannes.Breidenbach@nibio.no

Abstract

Fatalities associated with recreational activities occur every year as a result of snow avalanches. Terrain classification systems, such as the Avalanche Terrain Exposure Scale (ATES) are designed to provide guidance for safe route finding and this system has been automated (AutoATES). ATES classifies terrain into the three classes simple, challenging, and complex. Forests can provide some protection from avalanches, and these can be incorporated into avalanche hazard models. The objective of this study was to map relevant forest attributes (stem density and canopy cover) based on National Forest Inventory and remote sensing data and, subsequently, use these forest attributes as input to the AutoATES model to improve avalanche hazard maps. We predicted stem density with species-specific mixed-effects models and directly calculated canopy cover using airborne laser scanning data in a 20 Mha study area ranging from the arctic circle to southern Norway. We mapped these forest attributes for 16 m x 16 m pixels, which were used as input for the AutoATES model. The uncertainty of the stem number and canopy cover maps were 30% and 32%, respectively. The overall classification accuracy of 52 ski touring routes in Western Norway with a total length of 282 km increased by up to 12% when utilizing the mapped forest attributes, compared to the model without forest information. The F1 score for the three predicted ATES classes improved by up to 31%, 9%, and 6% for the three classes, respectively, when including a forest attribute in the AutoATES model. We conclude that large-scale fine-resolution forest attribute maps are valuable data in the modelling of avalanche hazards.

Keywords: Avalanches, Airborne laser scanning, remote sensing, National Forest Inventory, SR16

1 Introduction

Snow avalanches cause on average six fatalities per year in Norway (NGI 2022; Varsom 2022), these deaths and other injuries are primarily associated with recreation. Considerable resources have therefore been invested to reduce the number of casualties and hazard maps to assist route-finding are believed to be an important tool. Forest cover can alter avalanche behavior primarily by

38 modifying the snowpack through canopy interception (Bebi et al. 2001), but also to a lesser extent by
 39 increasing friction on prone slopes though the mechanism of the physical barriers of tree stems
 40 (Teich et al. 2014). On the other hand, large avalanches that release above the tree line are not
 41 affected by forests (Teich et al. 2012), these are more often a source of significant forest disturbance.
 42 Snow interception is largely dependent on tree species, because of the different morphology of tree
 43 crowns (i.e. branch structure, leaves or needles) and the size and number of trees in a given area,
 44 which are the factors that will collectively determine canopy cover and gaps. These parameters can
 45 potentially be derived from remote sensing in a way that is ideally suited to avalanche simulation
 46 (Brožová et al. 2020), the data are superior to traditional ground based inventory in this respect
 47 because they are spatially explicit. Maps of such forest attributes allow for monitoring of forest
 48 development and, subsequently, for adequate and effective forest management towards an
 49 optimized avalanche protection function to reduce avalanche hazards (Brang et al. 2006). This is
 50 especially crucial under the challenge of climate change that requires us to adapt forests to changing
 51 growing conditions to maintain healthy and resilient forests that can fulfil their functions.

52 Worldwide, various hazard maps have been developed for recreationalists using different avalanche
 53 classification schemes (Barbolini et al. 2011; Schudlach and Köhler 2016; Harvey et al. 2018; Larsen
 54 et al. 2020b). In Norway, the most used classification of avalanche terrain is the Avalanche Terrain
 55 Exposure Scale (ATES, Statham et al. 2006). The classification scheme divides avalanche terrain into
 56 simple (class 1), challenging (class 2) and complex (class 3) terrain (Table 1).

57 *Table 1: ATES Public Communication Model (v1.04) (Statham et al. 2006).*

| Description | Class | Terrain Criteria |
|-------------|-------|---|
| Simple | 1 | Exposure to low angle or primarily forested terrain. Some forest openings may involve the runout zones of infrequent avalanches. Many options to reduce or eliminate exposure. No glacier travel. |
| Challenging | 2 | Exposure to well defined avalanche paths, starting zones or terrain traps; options exist to reduce or eliminate exposure with careful route finding. Glacier travel is straightforward, but crevasse hazards may exist. |
| Complex | 3 | Exposure to multiple overlapping avalanche paths or large expanses of steep, open terrain; multiple avalanche starting zones and terrain traps below; minimal options to reduce exposure. Complicated glacier travel with extensive crevasse bands or icefalls. |

58

59 Originally, the ATES classification scheme was developed to provide an overall classification of an
 60 entire route based on the overall exposure likely to be encountered. Recent advances including
 61 modern cartographic techniques have made it more common to develop spatial maps. Making ATES
 62 maps, Delparte (2008) found that slope angle and forest density (number of trees per ha or stem
 63 density) were the two most important factors when classifying avalanche terrain with the ATES
 64 model. Campbell and Gould (2013) developed a specific model for spatial ATES including specific
 65 thresholds for slope angle and forest density. Building on the proposed model for spatial ATES
 66 mapping, (Larsen et al. 2020b, a) developed an automated ATES algorithm (AutoATES) for nationwide
 67 maps in Norway. However, due to limits in the spatial resolution and area-coverage of forest data the
 68 first version of the algorithm was only developed for non-forested terrain. The classification accuracy
 69 is consequentially most likely to be inaccurate below the treeline. While many recreational accidents
 70 associated with avalanches happen above the treeline, Norway is not a country with particularly high
 71 mountains and the fjordic landscape means that a considerable amount of avalanche prone terrain is
 72 found below the treeline. Therefore, the inclusion of forest attributes in terrain exposure

73 classification is important. Consequentially, in this study we aim to integrate high spatial resolution
74 data on forests into the spatially explicit classification of avalanche exposure.

75 Forest attributes can be mapped using remote sensing data when a relationship between remotely-
76 sensed variables and the forest attribute of interest exists. This relationship can be quantified via
77 regression models, where the response (a forest attribute) is explained by predictors (remote-
78 sensing variables). Such models are usually established using ground reference data from field plots
79 with known locations and remote-sensing data extracted for the same locations. This is commonly
80 known as the area-based approach (Næsset 2002). In Norway, the National Forest Inventory (NFI)
81 collects extensive information about forest properties in sample plots with a size of 250 m²
82 (Breidenbach et al. 2020a), which can serve as ground reference for remote-sensing data to establish
83 regression models predicting these forest attributes. Once established, these models can be
84 extrapolated to areas beyond field-inventory plots, to obtain prediction maps for the attribute or
85 attributes of interest. These predictions are particularly useful to support operational forest
86 management (reviewed by Brosofske et al. 2014). To achieve this mapping of forest attributes, the
87 entire area is gridded into aerial units of the same size as used for model fitting on NFI plots (250 m²),
88 and the same remote sensing variables are extracted for each unit. Following this approach, various
89 forest attributes were modelled and mapped for the Norwegian forest resource map SR16 (Astrup et
90 al. 2019; Hauglin et al. 2021), which is a national map at spatial resolution of 16 m x 16 m.

91 The necessary forest attributes for the AutoATES avalanche hazard model in Norway are canopy
92 cover or stem density. Canopy cover is defined as the proportion of the forest floor that is obscured
93 by tree crowns. Consequentially, airborne laser scanning (ALS) is almost the ideal way in which to
94 assess this because it can be directly obtained from discrete return laser scanner data as the
95 proportion of first returns above a specified height threshold, even though this method is slightly
96 biased in areas that are off the azimuth of the ALS scanner (Korhonen et al. 2011). On the other
97 hand, stem density is more challenging to obtain from wide-area coverage ALS because the lasers do
98 not penetrate the canopy with sufficient spatial-resolution to directly observe the stems. Therefore,
99 the aforementioned relationships need to be quantified. Previous studies have attempted to do this
100 in comparable forest types (Næsset and Bjerknes 2001; Lindberg et al. 2010; Lindberg and Hollaus
101 2012; Ene et al. 2012; Eysn et al. 2015). In general, the relative errors (based on RMSE) are quite high
102 and these increase with increasing complexity of the forest in terms of species and age structure. As
103 none of the currently available models are extrapolatable to the national level in Norway, this was an
104 important facilitating aim in the current study.

105 Our objectives were twofold: (I) to describe empirical models linking stem density (number of trees
106 per ha) by tree species observed at NFI sample plots to ALS metrics that are used to map these forest
107 attributes in a fine resolution of 16 m × 16 m; to map canopy cover obtained directly from ALS data;
108 and (II) to demonstrate and assess the inclusion of these in avalanche hazard classification models for
109 recreational activities. For the latter, we use the case studies of existing ski-touring routes in Western
110 Norway.

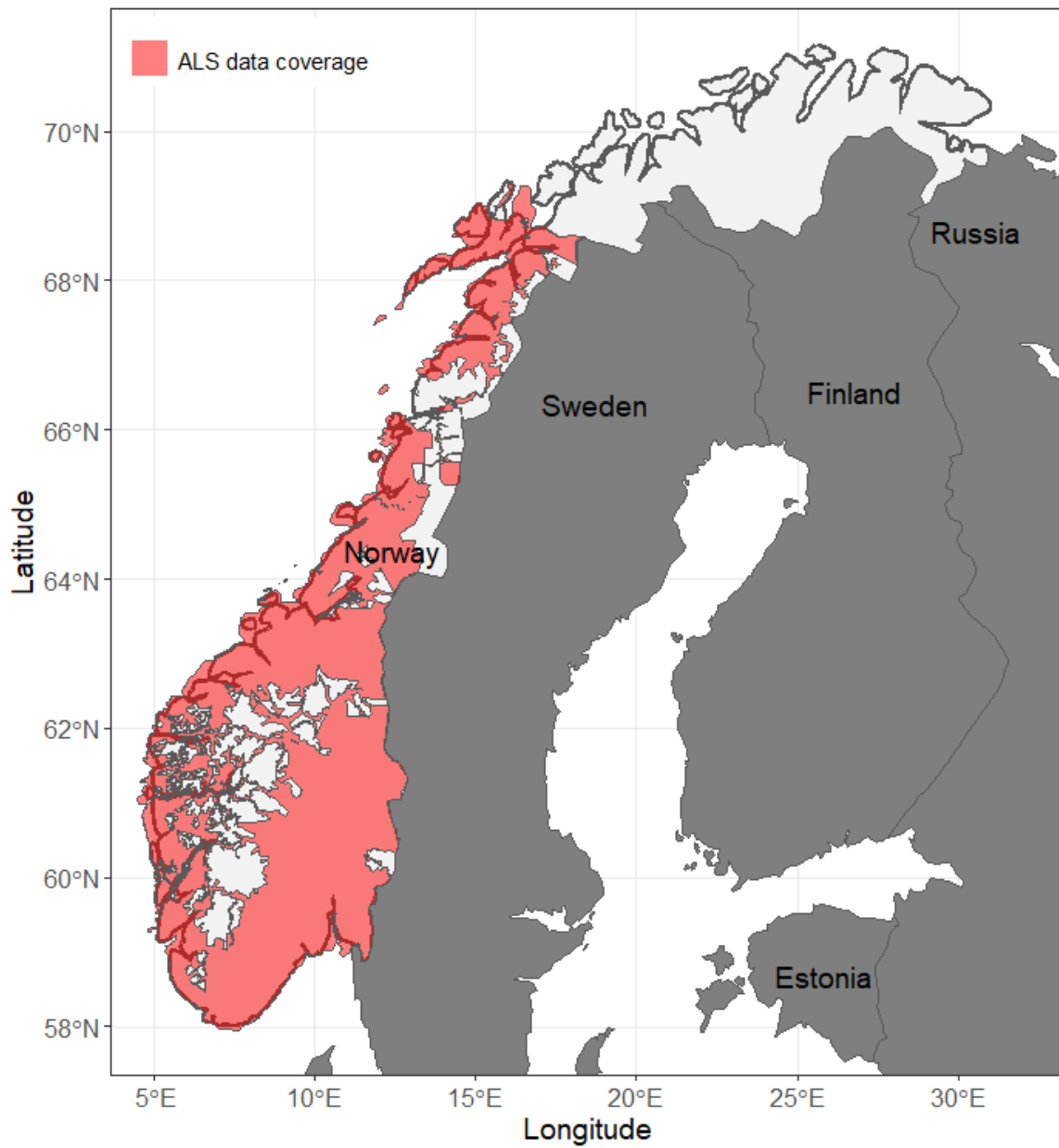
111 2 Material and methods

112 2.1 Study areas

113 In this study we referred to two different areas for the different analysis levels: modelling forest
114 attributes (large part of Norway), and modelling avalanche hazard for recreational activities
115 (mountainous hiking and skiing area).

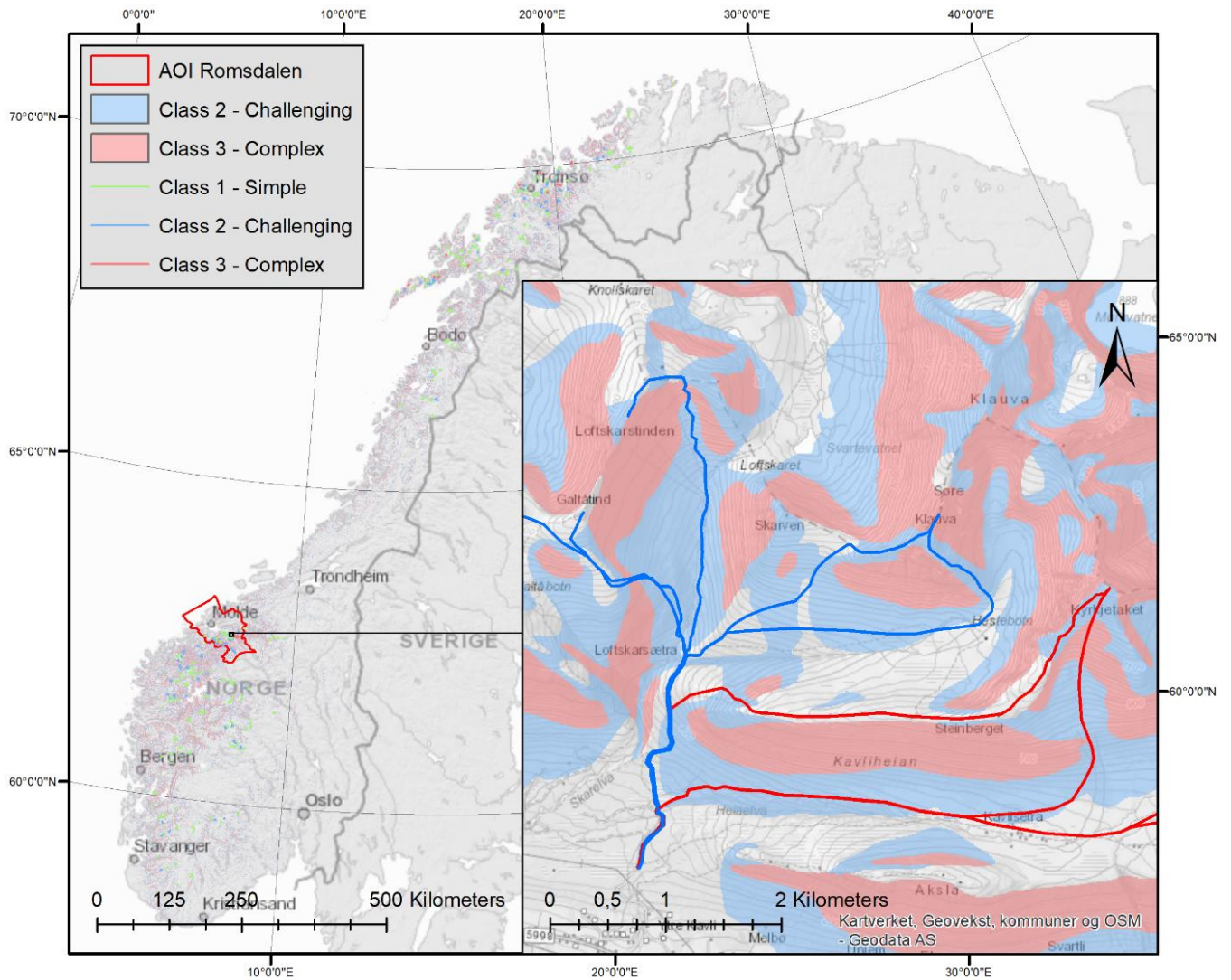
116 For modelling forest attributes with field reference data and auxiliary remote sensing data, we used
117 NFI data from a large part of the country covering 21.5 Mha (66% of the Norwegian mainland),

118 located in Norway between latitudes 58° and 69.5° N. This spatial extent was determined by the
119 availability of ALS data (Figure 1). Within the study area, forest growing conditions vary considerably
120 with latitude and elevation. The natural tree line is at around 1100 m asl in southern Norway and
121 around 130 m asl in the north. Depending on these factors, climate zones range roughly from
122 subarctic in the north and east, oceanic at the west coast, and continental in the south-east. The tree
123 species are primarily Norway spruce (*Picea abies*) and Scots pine (*Pinus sylvestris*). These make up
124 the majority of above ground biomass and standing volume. Birch (*Betula pendula* and *B. pubescens*)
125 is the most abundant species in terms of surface area and mainly occurs as early succession following
126 disturbance (including timber harvests) or in high elevation and/or latitude forests (Breidenbach et
127 al. 2020a). In this study the term broadleaves is used to represent what are mostly birch forests.
128 For assessing the effect of forest towards improved avalanche hazard models for recreational
129 activities we used the area of Romsdalen (Figure 2). This region is a popular destination for ski-
130 touring attracting national and international visitors. Within this area we focused on forested areas
131 on slopes that were relevant for avalanche hazard mapping along 52 documented ski-touring routes
132 (Table 2). The study area has an area of 3200 km² and the mountains reaches from sea level and up
133 to 1784 m above sea level.



134

135 *Figure 1: Study area with airborne laser scanner (ALS) data coverage used for modelling forest characteristics.*



136

137 *Figure 2: Romsdalen including ski-touring routes through mountainous terrain. The terrain and touring routes is*
 138 *classified according to the ATES classification scheme.*

139

140 *Table 2: Summary of the 52 documented ski-touring routes used in this study.*

| Manual ATES class | N routes | Total length (km) |
|-------------------|----------|-------------------|
| 1 | 12 | 43 |
| 2 | 26 | 131 |
| 3 | 14 | 108 |

141

142 2.2 Mapping forest attributes

143 To map the forest attribute stem density, we developed a mixed-modelling regression between this
 144 attribute (our response variable) and independent predictor variables calculated from remote
 145 sensing data. We used field measured stem density and visually interpreted canopy cover from the
 146 Norwegian National Forest Inventory (NFI, Breidenbach et al. 2020) as response variables, and
 147 remote sensing data from airborne laser scanning (ALS) and Sentinel-2 satellite images (S2) as
 148 independent predictor variables (sections 2.2.2 and 2.2.3). The attribute canopy cover could be

149 obtained from the ALS data directly. More details on this process can be found in Hauglin et al.
 150 (2021).

151

152 2.2.1 Data

153 National Forest Inventory data

154 We used the permanent sample plots of the Norwegian NFI as reference data (Breidenbach et al.
 155 2020a). In the study area, the NFI is based on a systematic grid of 3 km x 3 km in the lowland region
 156 and 3 km x 9 km in the low-productive, birch-dominated mountain region. For trees with a diameter
 157 at breast height ≥ 5 cm (dbh, 1.3 m above ground), parameters are measured on circular plots with
 158 a size of 250 m².

159 We used NFI plots located in stands dominated by spruce, pine, and birch (defined as plots with \geq
 160 75% timber volume of each tree species, respectively). From these plots, we only selected NFI plots
 161 in productive forest (yearly volume increment > 0.1 m³ / ha), and in one-layered forests, resulting in
 162 1,351 spruce, 1,064 pine, and 535 birch dominated plots that were used for modelling (Table 3).

163

164 *Table 3: Summary statistics of the Norwegian national forest inventory (NFI) data used for modelling in this*
 165 *study.*

| | Height (m) | Volume* (m ³) | Stem density** | Canopy cover (%) |
|-------------------|------------|---------------------------|----------------|------------------|
| overall | | | | |
| Min | 4.9 | 5.2 | 40 | 0 |
| Max | 34.1 | 1144.7 | 2840 | 99.0 |
| Mean | 15.2 | 208.9 | 860 | 68.5 |
| STD | 4.4 | 152.2 | 463 | 23.3 |
| Spruce | | | | |
| Min | 5.7 | 7.6 | 40 | 3.0 |
| Max | 34.1 | 1144.7 | 2840 | 99.0 |
| Mean | 17.0 | 277.1 | 1030 | 75.8 |
| STD | 4.4 | 172.2 | 451 | 19.5 |
| Pine | | | | |
| Min | 7.2 | 12.7 | 40 | 5.0 |
| Max | 28.3 | 693.7 | 2560 | 99.0 |
| Mean | 14.8 | 176.2 | 652 | 64.4 |
| STD | 3.5 | 106.2 | 370 | 22.0 |
| Broadleaved trees | | | | |
| Min | 4.9 | 5.2 | 40 | 0.0 |
| Max | 26.4 | 400.7 | 2760 | 99.0 |
| Mean | 11.3 | 101.7 | 845 | 60.2 |
| STD | 3.5 | 70.9 | 485 | 28.1 |

166 *Volume with bark; **number of trees ≥ 8 cm diameter at breast height (dbh) per ha.

167

168 Remote sensing data

169 ALS data were acquired during several measurement campaigns for the study area between 2010
 170 and 2019 with a density of 2 to 5 pulses per m². A high-resolution digital terrain model (DTM, 1 m x 1
 171 m pixel size) was produced from the last-return data by the Norwegian Mapping Authority

172 (Kartverket 2019). The ALS point cloud was height-normalized by subtracting the DTM elevation from
173 corresponding point cloud elevation using bi-directional interpolation. The height-normalized point
174 cloud was used to calculate various descriptive metrics for each NFI plot based on first returns, first
175 returns above 2 m height above ground, and last returns. The metrics included mean, variance,
176 coefficients of variation, kurtosis and skewness of ALS return heights, 10th, 25th, 50th, 75th, 90th, and
177 95th height percentiles, and ALS return density metrics for 10 height slices (d0 – d9). A canopy
178 coverage metric was calculated as percentage of first returns above 2 m (pctab2f). The DTM was
179 resampled to 16 m x 16 m, such that the cell size corresponded approximately to the area covered by
180 an NFI plot (250 m²). From the DTM, terrain slope was computed as a raster with a cell size of 16 m x
181 16 m. S2 bottom of atmosphere reflectance images acquired between 30 June and 31 July 2018 were
182 mosaiced using the bands B2, B3, B4, B5, B6, B7, B8, B8A, B11, and B12, measuring reflectance in the
183 visible, NIR and SWIR spectrum (Drusch et al. 2012). The normalized difference vegetation index
184 (NDVI) was calculated as band 8 minus band 4 divided by band 8 plus band 4 and tested as predictor
185 in the prediction models.

186

187 2.2.2 Modelling and mapping tree density

188 In the Norwegian forest resource mapping project SR16 (Astrup et al. 2019; Hauglin et al. 2021) linear
189 mixed regression models were developed estimating various forest properties. These models have
190 the structure:

$$191 \quad y = \mathbf{X}\beta + \mathbf{Z}u + \epsilon, \text{ with } u \sim N(0, \mathbf{G}) \text{ and } \epsilon \sim N(0, \mathbf{R}), \quad (\text{Equation 1})$$

192 where y is the dependent response variable, \mathbf{X} and \mathbf{Z} are the design matrices for fixed and random
193 effects, respectively, β are the fixed effects parameters, u is a vector of random effects, and \mathbf{G} and \mathbf{R}
194 are the covariance matrices for random effects and residual errors, respectively. We used the nlme
195 package (Pinheiro et al. 2020) in the statistics software R (R Core Team 2020) to estimate the model
196 parameters. A starting model was stepwise reduced by forward and backward selection of predictors
197 based on Akaike Information Criterion as stopping rule (stepAIC function in R (Venables and Ripley
198 2002)) and was further reduced by backward selection based on p-values ($p < 0.05$). We used the
199 information on ALS project acquisition as random effect on slope in the models to account for
200 differences in ALS data collection between the different projects.

201 We used the approach described above and the model structure in equation 1 to fit linear-mixed
202 effects models predicting stem density (for trees ≥ 8 cm dbh) for three tree species of interest. Area
203 wide predictions of the forest attributes were made by applying the developed models to 16 m x 16
204 m pixels, which is similar to the area of the NFI plots used during model fitting. A tree species map
205 (Breidenbach et al. 2020b) was used to apply the corresponding tree species specific model.

206

207 2.2.3 Mapping canopy cover

208 Canopy cover was calculated from the ALS data directly by analyzing the spatial distribution of laser
209 echoes with above-ground heights ≥ 5 m. The normalized laser point cloud of each 16 m x 16 m
210 pixel was divided into 64 voxels of size $2 \times 2 \times h$ m³, where h is the vertical distance from 5 m above
211 ground to the maximum above-ground echo height. Each voxel was thus defined by a 2×2 m² base
212 at 5 m above ground and extended upwards to the height of the highest echo, i.e., h . Note that this
213 means that the shape of the voxels were in most cases not cubical, but typically was higher than the
214 2 m sides of the base. The proportion of non-empty voxels were used as a representation for canopy

215 cover in the 16 m × 16 m pixel, with non-empty voxels being voxels containing at least one laser
 216 echo. Canopy cover was then compared to field-based estimates of canopy cover at NFI plots.

217

218 2.3 Avalanche hazard maps for recreational activities

219 To investigate the effect of forest data on recreational avalanche maps, we ran AutoATES using both
 220 canopy cover and stem density and compared it to AutoATES with no forest data as input (Larsen et
 221 al. 2020b, a). AutoATES is an automated algorithm that is made to create spatial ATES maps using
 222 only a DEM and forest data (optional) as input. The first step of the algorithm is to calculate the
 223 potential release areas (PRA) using the algorithm developed by Veitinger et al. (2016) and later
 224 modified by Sharp (2018). Using a fuzzy operator, they combine the slope angle, terrain roughness,
 225 wind shelter and forest data into a raster layer ranging from 0 to 1, where 1 is a very likely release
 226 area, and 0 is not likely (Veitinger et al. 2016; Sharp 2018). When the PRA layer is completed, a
 227 runout model is used to calculate areas downslope of the PRAs that could be affected by an
 228 avalanche. In Larsen et al. (2020b) the TauDEM model is being used (Tarboton 2004), but recent
 229 advances show that the new FlowPy model (D’Amboise et al. 2021) is much better suited (Larsen et
 230 al. 2020a). Both models use a flow model that is limited by the angle of reach, which is the angle
 231 from the PRA to the lowermost point in the flow model. In this paper, we only use the best
 232 performing algorithm utilizing FlowPy. The improved algorithm can be tuned using different
 233 thresholds for slope angle (SAT), cell count (CC), angle of reach (AAT), PRA threshold (PRA THD) and
 234 forest density. To test whether the forest input data improves the result of the AutoATES model, we
 235 used a fixed set of thresholds except for forest data (Table 4).

236 *Table 4: The input parameters used for AutoATES. The parameters were held constant between the models that included no*
 237 *forest data, stem density and canopy cover data.*

| Parameter: | AAT1 | AAT2 | AAT3 | CC1 | CC2 | SAT01 | SAT12 | SAR23 | SAT34 | PRA THD |
|------------|------|------|------|-----|-----|-------|-------|-------|-------|---------|
| Value: | 20° | 25° | 31° | 50 | 250 | 15° | 25° | 31° | 37° | 0.15 |

238

239 A fuzzy membership value also has to be set for each forest density type used in the PRA calculation.
 240 The value is defined using a Cauchy membership value given by the function $\mu(x)$ (Jang et al. 1997).

241
$$\mu(x) = \frac{1}{1 + \left(\frac{x-c}{a}\right)^{2b}} \quad \text{(Equation 2)}$$

242 where x is the weighting of the forest attribute vs. slope angle, roughness and wind shelter in the
 243 fuzzy operator (Veitinger et al. 2016; Sharp 2018). The remaining parameters are described in Table
 244 5. Sharp (2018) defined the membership values for stem density, while we suggest new preliminary
 245 membership values for canopy cover (Table 5).

246

247 *Table 5: The parameters used to calculate the fuzzy membership of forest input in the PRA model.*

| Parameter: | a | b | c |
|-----------------------------------|-----|-----|------|
| Stem density (Sharp et al., 2018) | 350 | 2.5 | -150 |
| Canopy cover | 240 | 25 | -200 |

248

249 As a basis for comparison in the case study area we considered the classification of routes by local
 250 avalanche experts. The dataset consists of a set of 52 routes with a total length of 282 km that were
 251 manually mapped by local avalanche experts working for NVE (Larsen et al. 2020b) in 2018. The work

252 was done using the ATES v1.04 defined by Statham et al. (2006). Methods used included: a GIS web
253 tool, visual interpretation of aerial imagery, local expertise, and field surveys. Each route is classified
254 according to eleven different avalanche terrain factors and classified as either simple, challenging, or
255 complex terrain. If the route is within the challenging or complex definition of slope angle for a short
256 section of the trip, the whole trip will be classified as challenging or complex. Therefore, it is
257 important to note that there is a difference between the manual ATES classification of linear routes
258 and the spatial AutoATES classification of 10 m x 10 m pixels (Larsen et al. 2020a). The manual ATES
259 classification considers the trajectory of the whole route, while the AutoATES algorithm outputs a
260 classification value for each pixel. To compare the manual ATES classification with the AutoATES
261 classification, the AutoATES map was sampled every 10 m along the length of the route. The 95th
262 percentile of the extracted AutoATES predictions was used to assign one predicted class per route.
263 We calculated weighted accuracies using lengths of classified routes.

264

265 3 Results

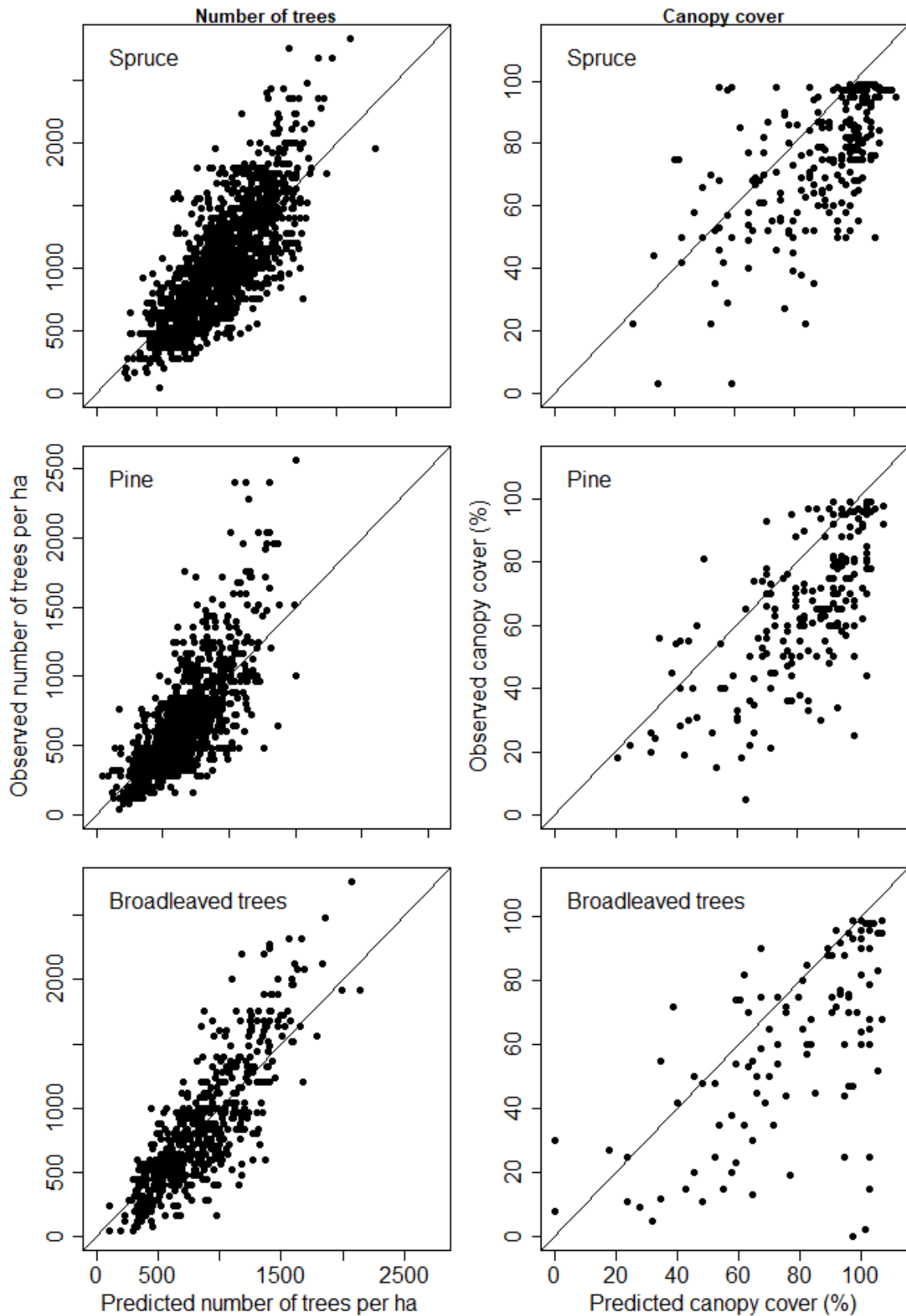
266 3.1 Forest attribute maps

267 We successfully modelled the stem density using linear mixed effects models, and directly calculated
268 canopy cover from ALS data for the spruce, pine, and birch forests (Figure 3). The fit statistics
269 associated with the linear-mixed models for stem density showed the results for spruce were the
270 most accurate in terms of RMSE (Table 6). The significant predictors were similar for the spruce and
271 pine models. Both models contained the 75th percentile of first ALS returns, (h75f) and its squared
272 version (h75fsq), the percentage of first ALS returns above 2 m height, (pctab2f) and its squared
273 version (pctab2fsq), the interactions between h75f and pctab2f, and between h75fsq and pctab2fsq,
274 the normalized difference vegetation index (NDVI), and terrain slope. For the spruce model one
275 additional first return density metric d6f was included, and for the pine model the first return density
276 metric d4f was included. The model for birch forests only included the predictors h75fsq, pctab2fsq,
277 and d6f. The model details can be found in Table 9 in the appendix.

278

279

280



281

282 *Figure 3: Results of models for stem density (number of trees per ha, left column), and canopy cover directly*
 283 *from laser scanner data (right column); all attributes were stratified into three tree species groups: spruce (top*
 284 *row), pine (middle row), and broadleaved trees (bottom row).*

285

286 Canopy cover directly obtained from the ALS data as described in the Methods section showed a
 287 good fit with canopy cover values from the NFI data (Figure 3, Table 6). We also compared canopy
 288 cover calculated as proposed by Korhonen et al. (2011) with canopy cover from the NFI. However,
 289 this relationship was worse and therefore not further considered in this study.

290

291 *Table 6: Characteristics of the fitted models and canopy cover relationship*

| | Stem density | Canopy cover |
|-----------------------|--------------|--------------|
| Norway spruce | | |
| Pseudo R ² | 0.59 | - |
| RMSE _{cv} | 307.9 | 21.0 |
| RMSE _{cv} % | 29.9 | 31.5 |
| Variance components % | | |
| Fixed effects | 50.91 | - |
| Random effect | 5.59 | - |
| Residual | 43.50 | - |
| Scots pine | | |
| Pseudo R ² | 0.56 | - |
| RMSE _{cv} | 277.4 | 23.9 |
| RMSE _{cv} % | 42.5 | 37.1 |
| Variance components % | | |
| Fixed effects | 40.72 | - |
| Random effect | 10.81 | - |
| Residual | 48.47 | - |
| Broadleaved trees | | |
| Pseudo R ² | 0.68 | - |
| RMSE _{cv} | 330.7 | 29.2 |
| RMSE _{cv} % | 39.1 | 39.6 |
| Variance components % | | |
| Fixed effects | 48.08 | - |
| Random effect | 13.99 | - |
| Residual | 37.93 | - |

292

293

294 3.2 Assessment of hazard maps for recreational activities

295 Due to the inherent differences in scale between the route-level reference and the pixel-level
 296 predictions we can only make a meaningful comparison for reference classes 1 and 2 and predicted
 297 classes 2 and 3 (see methods description in section 2.3). For comparison of all classes, we made
 298 additional analyses on route-level by summarizing pixel-level predictions for each route.

299 Overall, including forest attributes in the AutoATES model improved terrain and, thereby, route
 300 classifications with regard to avalanche hazard. Using the 95th percentile of predicted values to assign
 301 one class per route, AutoATES-Forest classifications showed a considerable improvement compared
 302 to AutoATES without forest attribute (Table 7).

303

304 *Table 7: Confusion matrices for 282 km manually classified routes (ATES) in Romsdalen and the automated ATES*
 305 *algorithms AutoATES, AutoATES-Forest (canopy cover) and AutoATES-Forest (stem density) on entire-route*

306 level. Routes were classified according to the 95th percentile of AutoATES and AutoATES-Forest predictions.
 307 Values represent km of routes (route count is given in brackets).

| <u>No forest parameters included</u> | | AutoATES | | |
|--------------------------------------|---------------------|-----------------|-----------|-----------|
| | | Class 1 | Class 2 | Class 3 |
| Manually mapped (ATES) | Class 1 simple | 10.5 (3) | 21.8 (7) | 10.6 (2) |
| | Class 2 challenging | 0 (0) | 59.9 (12) | 71.2 (14) |
| | Class 3 complex | 0 (0) | 23.1 (3) | 84.7 (11) |

| <u>Including canopy cover</u> | | AutoATES-Forest | | |
|-------------------------------|---------------------|------------------------|-----------|-----------|
| | | Class 1 | Class 2 | Class 3 |
| Manually mapped (ATES) | Class 1 simple | 23.1 (6) | 13.8 (5) | 6.0 (1) |
| | Class 2 challenging | 0 (0) | 90.1 (16) | 41.0 (10) |
| | Class 3 complex | 0 (0) | 31.9 (4) | 75.8 (10) |

| <u>Including stem density</u> | | AutoATES-Forest | | |
|-------------------------------|---------------------|------------------------|-----------|----------|
| | | Class 1 | Class 2 | Class 3 |
| Manually mapped (ATES) | Class 1 simple | 29.2 (8) | 13.7 (4) | 0 (0) |
| | Class 2 challenging | 24.7 (3) | 78.9 (16) | 27.5 (7) |
| | Class 3 complex | 0 (0) | 38.7 (5) | 69.0 (9) |

308

309 Overall accuracies weighted by route lengths increased from 0.55 for AutoATES to 0.67 for AutoATES-
 310 Forest using canopy cover and to 0.63 for AutoATES-Forest using stem density. Similarly, also the
 311 other accuracy statistics F1 score, Sensitivity, and Precision improved (Table 8). Only sensitivity of
 312 class 3 decreased when using forest properties in the model since more routes that were marked as
 313 class 3 in the reference were predicted as class 2.

314

315 *Table 8: accuracies for routes assigned to one class; routes were assigned one predicted value using the 95th percentile of*
 316 *predicted pixel values within a route; OA = Overall accuracy, PA = Producer's accuracy, UA = User's accuracy, PPV = positive*
 317 *predictive value.*

| | OA | F1 score | | | Sensitivity/Recall (PA) | | | Precision/PPV (UA) | | |
|--------------------------|------|----------|---------|---------|-------------------------|---------|---------|--------------------|---------|---------|
| | | Class 1 | Class 2 | Class 3 | Class 1 | Class 2 | Class 3 | Class 1 | Class 2 | Class 3 |
| AutoATES No forest | 0.55 | 0.39 | 0.51 | 0.62 | 0.25 | 0.46 | 0.79 | 1.00 | 0.57 | 0.51 |
| AutoATES Canopy cover | 0.67 | 0.70 | 0.58 | 0.66 | 0.54 | 0.69 | 0.70 | 1.00 | 0.66 | 0.62 |
| AutoATES Stem density | 0.63 | 0.60 | 0.60 | 0.68 | 0.68 | 0.60 | 0.64 | 0.54 | 0.60 | 0.72 |

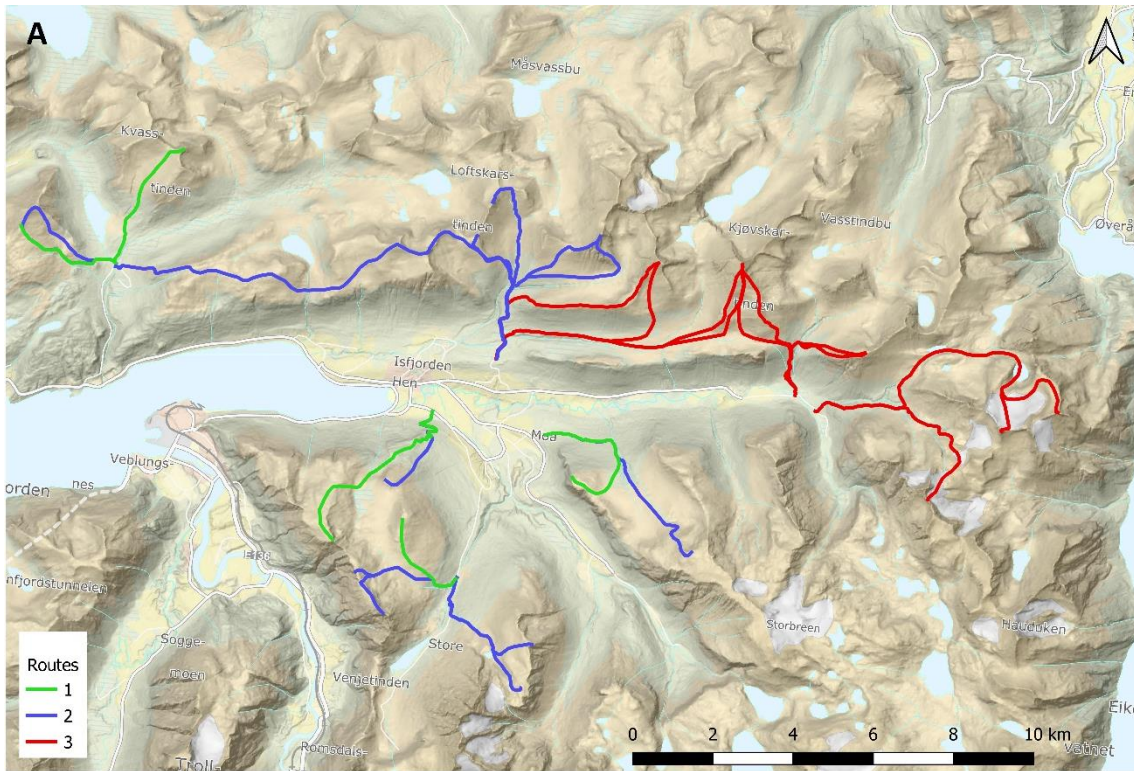
318

319

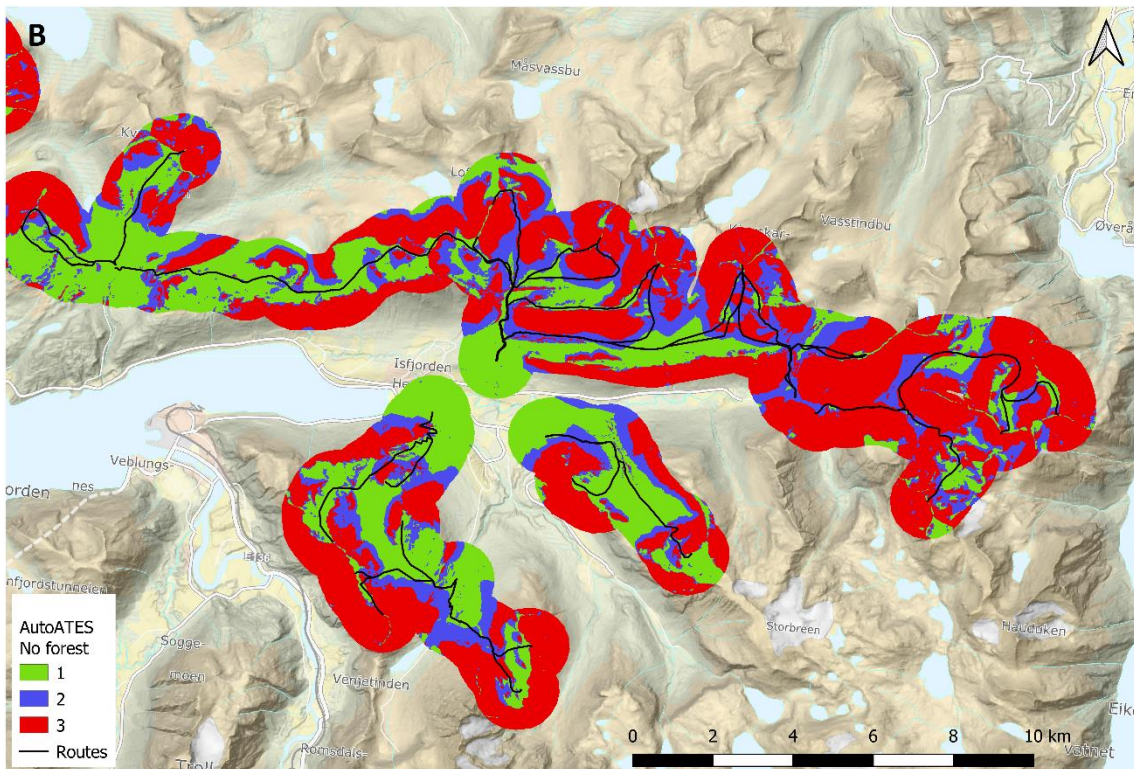
320

321

322

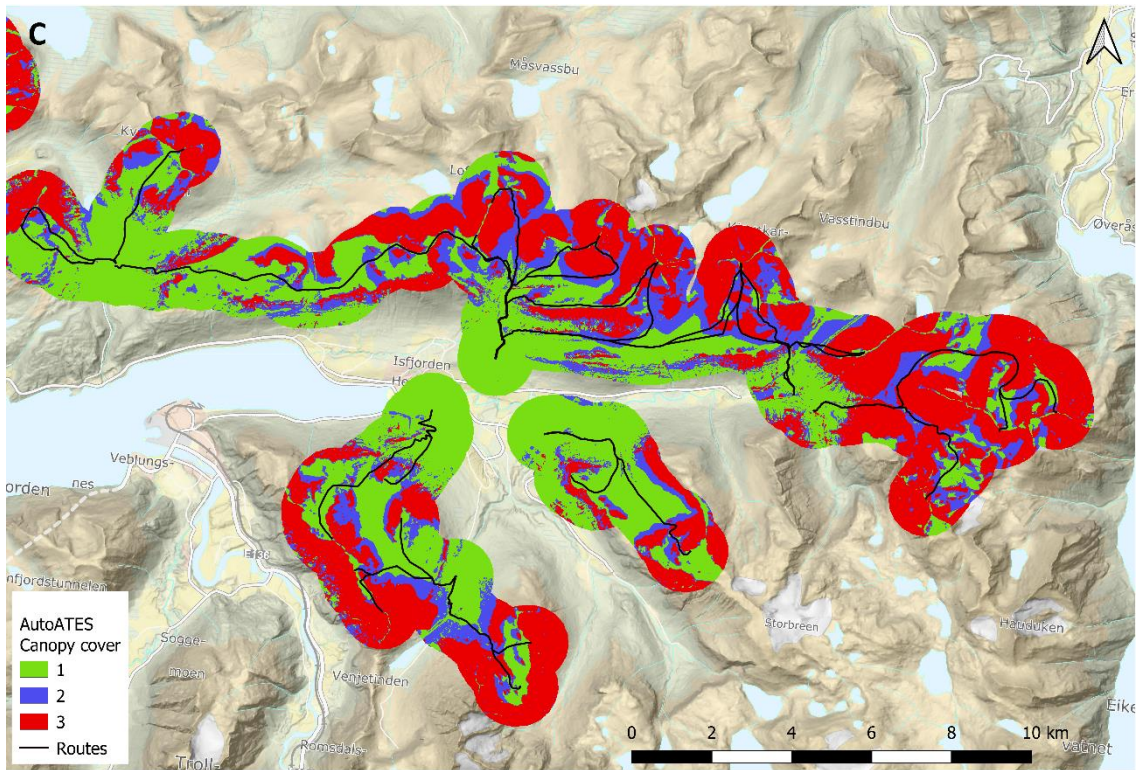


324

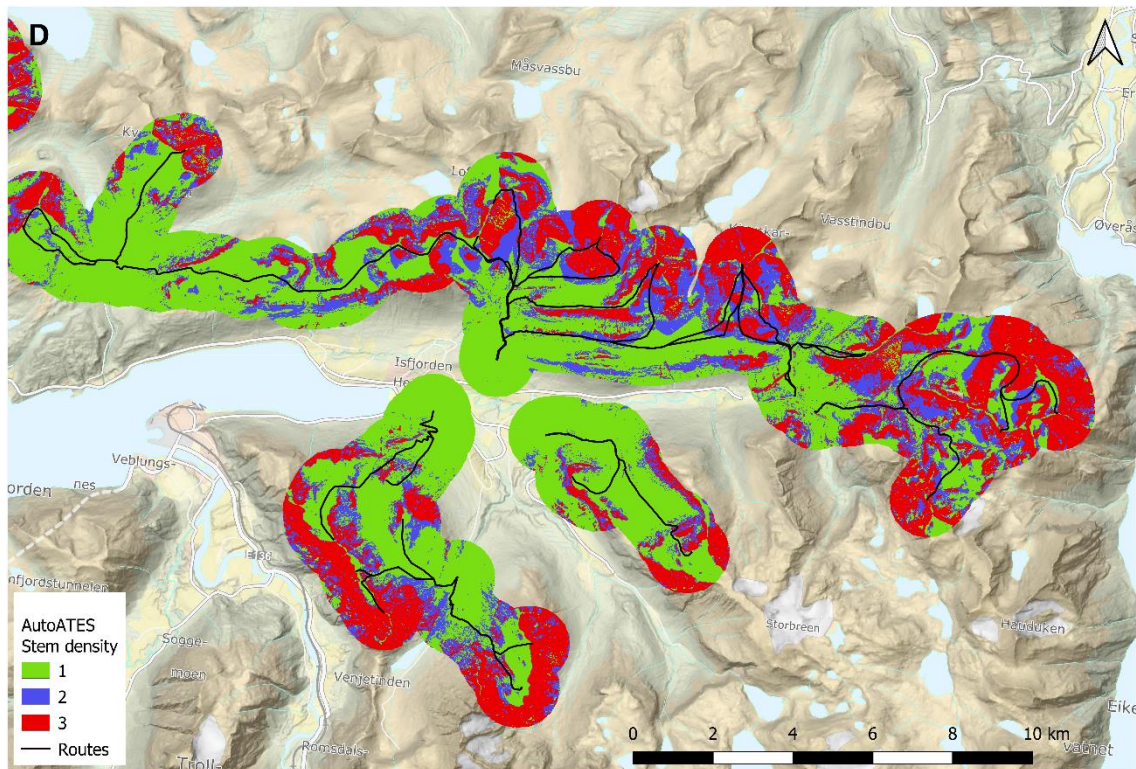


325

326 *Figure 4: Area around the town Isfjorden; A) manually ATES classification of touring routes according to the part*
 327 *with the greatest hazard used as reference; B) output of AutoATES model without forest; C) output of AutoATES-*
 328 *Forest model with forest canopy cover as model input; D) output of AutoATES-Forest model with forest stem*
 329 *density as model input.*



330



331

332 *Figure 4 continued.*

333

334

335 4 Discussion and Conclusion

336 In this study we successfully modelled and estimated the forest attributes of stem density and
337 canopy cover respectively using NFI and remote sensing data collected over a large area in Norway
338 encompassing various growing conditions. We could produce maps of these attribute and include
339 them as inputs in the spatially explicit avalanche hazard model AutoATES-Forest in order to improve
340 avalanche hazard maps for recreational activities.

341 We found that the forest attribute stem density could be modeled with relatively high accuracy using
342 remote sensing data and observed coefficient of determination (pseudo R^2) values of 0.59, 0.56, and
343 0.68 for Norway spruce, Scots pine, and broadleaved trees, respectively. Cross-validated RMSEs were
344 308 (30%), 277 (43%), and 331 (39%) for Norway spruce, Scots pine, and broadleaved trees,
345 respectively. Tompalski et al. (2019) found similar results with R^2 and RMSE of 0.37 and 293 (42%),
346 respectively, for modelling stem density in Canada. Lindberg and Hollaus (2012) compared area-
347 based and single tree-based approaches for estimating the number of trees and found RMSE of 53%
348 (area-based) and 63-92% (single tree based). Ene et al. (2012) used the single tree-based approach
349 and reported 46-50% detection rate for stem number estimates in heterogenous boreal forests. Eysn
350 et al. (2015) reported 47% overall tree detection rate in heterogenous alpine forest. Stem density is
351 difficult to predict using the type of remote sensing data used in this study and the area-based
352 approach. While using very high-resolution ALS or drone data would allow for analyses on single tree
353 level that might result in higher accuracies, collecting such high-resolution data for the single tree
354 approach on such a large spatial scale used in this study is practically not feasible. In addition to the
355 area that needs to be covered, forests are dynamic ecosystems and their structure changes from
356 year to year, therefore it is not a matter of once off acquisition but rather regular monitoring. We
357 have therefore tried to consider approaches that can make use of data collected in regular surveys,
358 but for areas of particular concern, higher-resolution data might still be appropriate to guide forest
359 management.

360 We estimated canopy cover in a slightly different way as proposed by Korhonen et al. (2011). Our
361 voxel-based approach with a height threshold of 5 m showed a better correlation with canopy cover
362 obtained by the NFI than canopy cover calculated according to Korhonen et al. (2011). The relation
363 between predicted and observed canopy cover was not as good as for the other forest attribute stem
364 density. This can partially be attributed to the fact that canopy cover in the NFI is not measured, but
365 visually estimated by the NFI crew in five percent steps. Therefore, the ground-truth could be argued
366 to be less reliable than the aerial measurement.

367 Using the forest attributes stem density or canopy cover in the AutoATES-Forest models improved
368 the terrain and route hazard classification compared to the AutoATES model without forest
369 attributes. The percentage of class 1 (simple terrain) wrongly classified as class 2 (challenging) or 3
370 (complex) was reduced. When classifying ski-touring routes linearly using manual ATES, the overall
371 class is decided by the most hazardous area on a given route. This means that if the route is located
372 in mostly simple terrain (class 1), the whole route could be classified as complex terrain (class 3) if
373 there is a short section of this type of terrain along the given route. This is a deliberate design feature
374 that errs on the side of safety. A result of this is that even though the algorithm, which works on the
375 pixel level, defines a large percentage of a given route as less hazardous than the manual
376 classification class rating, it is not necessarily wrong. When assigning one hazard class to each route
377 according to the 95th percentile of pixel values from the AutoATES predictions, the overall accuracy
378 increased from 55% (AutoATES) to 67% (AutoATES-Forest canopy cover) and to 63% (AutoATES-
379 Forest stem density). Using the forest attribute canopy cover appeared to result in slightly better
380 classifications, but the difference between the two forest metrics was not as great as the difference

381 between the use of forest metrics and the lack of forest metrics. These results indicate that adding
382 spatially explicit information on forest attributes are beneficial for terrain evaluation. Other forest
383 properties such as diameter distributions can be estimated and mapped from laser scanner data
384 (Räty et al. 2021) and should be considered as in put to avalanche hazard models. Furthermore,
385 avalanche hazard models can be further developed to use forest properties are used as continuous
386 values as input.

387 Brožová et al. (2020) evaluated variables extracted from ALS and photogrammetric point clouds
388 towards their influence on simulation results of avalanche runout. Remote sensing based tree
389 heights, canopy coverage, and DTM roughness were used for avalanche simulation. They concluded
390 that remote sensing data with a fine resolution of about 1 m x 1 m were generally suitable to model
391 relevant forest attributes used as input for avalanche simulation. The simulation results using the
392 two data sources - ALS and photogrammetric point clouds – were both sufficiently accurate for
393 numerical modelling and for real-world applications in snow avalanche hazard mapping. Bühler et al.
394 (2022) described automated avalanche hazard mapping using the RAMMS model in one Canton in
395 Switzerland. Terrain slope and the forest properties percentage of crown cover and gap width were
396 used to predict an avalanche release probability for each forested raster cell of 5 m x 5 m. This was
397 used as input into the avalanche model. Similar to the present study the authors deduced threshold
398 values for forest properties that entered the model.

399 A wider implication of these findings is that the value of ecosystem services, such as the protection
400 function of forests, is often difficult to assess. In this respect, our study showed the positive effect of
401 forest in avalanche hazard prediction, and this is something that can be quantified, at least spatially.
402 The authors jointly consider that no price should be put on human lives and therefore we will not
403 enter into discussion of the monetary value of such protection here, though examples exist (e.g Grilli
404 et al. 2020) and it is no doubt an important subject for forest owners whose primary interests are
405 timber revenues. In this respect however, we feel that protection should influence forest
406 management decisions, but that significantly more research is required to investigate optimal forest
407 management of protective forests in a Norwegian context. Finally, models and maps based on those
408 models are only predictions. Predicting and mapping the probability of avalanche releases is meant
409 as an additional planning aid for route choice, much like a weather forecast, and they can be wrong.
410 Avalanche conditions change dramatically depending on snow conditions and these are not in any
411 way included in the ATES system. While we strive to improve the decision-making tools, these are no
412 substitute local evaluation of the current conditions on the ground, and this requires specific training
413 and experience. Even then, avalanches pose a significant threat and safety is solely the responsibility
414 of the individual. Nonetheless, we can conclude that the inclusion of forest attributes in avalanche
415 hazard models can considerably improve their predictive performance.

416

417 5 Acknowledgements

418

419

420

421

422 6 Appendix

423

424 *Table 9: stem density models; coefficients, their standard errors, and p-values for the tree species specific linear*
 425 *regression models for spruce, pine, and broadleaved trees.*

| Variable | Estimate | Std. Error | p-value |
|---|----------|------------|---------|
| Stem density model for spruce | | | |
| <i>Intercept</i> | -73.85 | 130.87 | 0.573 |
| <i>h75f</i> | 37.52 | 23.48 | 0.110 |
| <i>h75fsq</i> | -1.37 | 0.65 | 0.034 |
| <i>pctab2f</i> | -175.99 | 406.92 | 0.665 |
| <i>pctab2fsq</i> | 1862.63 | 421.25 | < 0.001 |
| <i>d6f</i> | 1122.08 | 103.12 | < 0.001 |
| <i>NDVI</i> | 414.73 | 113.61 | < 0.001 |
| <i>slope</i> | -1.94 | 0.57 | < 0.001 |
| <i>h75f_x_pctab2f</i> | -89.52 | 35 | 0.011 |
| <i>h75fsq_x_pctab2fsq</i> | 1.57 | 0.74 | 0.033 |
| Stem density model for pine | | | |
| <i>Intercept</i> | -171.32 | 109.02 | 0.116 |
| <i>h75f</i> | 16.39 | 15.27 | 0.283 |
| <i>h75fsq</i> | 0.60 | 0.65 | 0.361 |
| <i>pctab2f</i> | 364.46 | 421.98 | 0.388 |
| <i>pctab2fsq</i> | 1491.58 | 375.16 | < 0.001 |
| <i>d4f</i> | 986.33 | 140.30 | < 0.001 |
| <i>NDVI</i> | 240.69 | 110.80 | 0.03 |
| <i>Slope</i> | -1.84 | 0.54 | 0.001 |
| <i>h75f x pctab2f</i> | -126.86 | 32.79 | < 0.001 |
| <i>h75fsq x pctab2fsq</i> | 2.37 | 0.84 | 0.005 |
| Stem density model for broadleaved trees | | | |
| <i>Intercept</i> | 191.58 | 41.93 | < 0.001 |
| <i>h75fsq</i> | -2.07 | 0.25 | < 0.001 |
| <i>pctab2fsq</i> | 1255.46 | 91.02 | < 0.001 |
| <i>d6f</i> | 993.70 | 180.47 | < 0.001 |

426

427

428 7 References

429 Astrup R, Rahlf J, Bjørkelo K, et al (2019) Forest information at multiple scales: development,
 430 evaluation and application of the Norwegian forest resources map SR16. *Scand J For Res* 0:1–
 431 13. <https://doi.org/10.1080/02827581.2019.1588989>

432 Barbolini M, Pagliardi M, Ferro F, Corradeghini P (2011) Avalanche hazard mapping over large
 433 undocumented areas. *Nat Hazards* 56:451–464. <https://doi.org/10.1007/s11069-009-9434-8>

434 Bebi P, Kienast F, Schönenberger W (2001) Assessing structures in mountain forests as a basis for
 435 investigating the forests' dynamics and protective function. *For Ecol Manage* 145:3–14.
 436 [https://doi.org/10.1016/S0378-1127\(00\)00570-3](https://doi.org/10.1016/S0378-1127(00)00570-3)

437 Brang P, Schönenberger W, Frehner M, et al (2006) Management of protection forests in the
 438 European Alps: an overview

439 Breidenbach J, Granhus A, Hysten G, et al (2020a) A century of National Forest Inventory in Norway –
440 informing past, present, and future decisions. For Ecosyst 7:. [https://doi.org/10.1186/s40663-](https://doi.org/10.1186/s40663-020-00261-0)
441 [020-00261-0](https://doi.org/10.1186/s40663-020-00261-0)

442 Breidenbach J, Waser LT, Debella-Gilo M, et al (2020b) National mapping and estimation of forest
443 area by dominant tree species using Sentinel-2 data. Under Prep

444 Brosofske KD, Froese RE, Falkowski MJ, Banskota A (2014) A review of methods for mapping and
445 prediction of inventory attributes for operational forest management. For. Sci. 60:733–756

446 Brožová N, Fischer JT, Bühler Y, et al (2020) Determining forest parameters for avalanche simulation
447 using remote sensing data. Cold Reg Sci Technol 172:.
448 <https://doi.org/10.1016/j.coldregions.2019.102976>

449 Bühler Y, Bebi P, Christen M, et al (2022) Automated avalanche hazard indication mapping on state
450 wide scale. Nat Hazards Earth Syst Sci Discuss 2022:1–22. [https://doi.org/10.5194/nhess-2022-](https://doi.org/10.5194/nhess-2022-11)
451 [11](https://doi.org/10.5194/nhess-2022-11)

452 Campbell C, Gould B (2013) A proposed practical model for zoning with the Avalanche Terrain
453 Exposure Scale. In: International Snow Science Workshop. Grenoble - Chamonix Mont-Blanc

454 D’Amboise CJL, Neuhauser M, Teich M, et al (2021) Flow-Py v1.0: A customizable, open-source
455 simulation tool to estimate runout and intensity of gravitational mass flows. Geosci Model Dev
456 Discuss 2021:1–28. <https://doi.org/10.5194/gmd-2021-277>

457 Delparte DM (2008) Avalanche Terrain Modeling in Glacier National Park, Canada. University of
458 Calgary (Canada)

459 Drusch M, Del Bello U, Carlier S, et al (2012) Sentinel-2: ESA’s Optical High-Resolution Mission for
460 GMES Operational Services. Remote Sens Environ 120:25–36.
461 <https://doi.org/10.1016/j.rse.2011.11.026>

462 Ene L, Næsset E, Gobakken T (2012) Single tree detection in heterogeneous boreal forests using
463 airborne laser scanning and area-based stem number estimates. Int J Remote Sens 33:5171–
464 5193. <https://doi.org/10.1080/01431161.2012.657363>

465 Eysn L, Hollaus M, Lindberg E, et al (2015) A benchmark of lidar-based single tree detection methods
466 using heterogeneous forest data from the Alpine Space. Forests 6:1721–1747.
467 <https://doi.org/10.3390/f6051721>

468 Grilli G, Fratini R, Marone E, Sacchelli S (2020) A spatial-based tool for the analysis of payments for
469 forest ecosystem services related to hydrogeological protection. For Policy Econ 111:102039.
470 <https://doi.org/10.1016/j.forpol.2019.102039>

471 Harvey S, Schudlach G, Bühler Y, et al (2018) Avalanche terrain maps for backcountry skiing in
472 Switzerland. In: International Snow Science Workshop Proceedings. Innsbruck, Austria, pp
473 1625–1631

474 Hauglin M, Rahlf J, Schumacher J, et al (2021) Large scale mapping of forest attributes using
475 heterogeneous sets of airborne laser scanning and National Forest Inventory data. For Ecosyst
476 8:65. <https://doi.org/10.1186/s40663-021-00338-4>

477 Jang JSR, Sun CT, Mizutani E (1997) Neuro-fuzzy and soft computing: a computational approach to
478 learning and machine intelligence. IEEE Trans Automat Contr 42:

479 Kartverket (2019) Høydedata og terrengmodeller for landområdene.
480 <https://www.kartverket.no/data/Hoydedata-og-terrengmodeller/>. Accessed 11 Mar 2020

481 Korhonen L, Korpela I, Heiskanen J, Maltamo M (2011) Airborne discrete-return LIDAR data in the
482 estimation of vertical canopy cover, angular canopy closure and leaf area index. *Remote Sens*
483 *Environ* 115:1065–1080. <https://doi.org/10.1016/j.rse.2010.12.011>

484 Larsen HT, Hendriks J, Schauer A, et al (2020a) Development of Automated Avalanche Terrain
485 Exposure Scale Maps: Current and Future. In: *Virtual Snow Science Workshop 2020*

486 Larsen HT, Hendriks J, Slåtten MS, Engeset R V. (2020b) Developing nationwide avalanche terrain
487 maps for Norway. *Nat Hazards* 103:2829–2847. <https://doi.org/10.1007/s11069-020-04104-7>

488 Lindberg E, Hollaus M (2012) Comparison of Methods for Estimation of Stem Volume, Stem Number
489 and Basal Area from Airborne Laser Scanning Data in a Hemi-Boreal Forest. *Remote Sens.* 4

490 Lindberg E, Holmgren J, Olofsson K, et al (2010) Estimation of tree lists from airborne laser scanning
491 by combining single-tree and area-based methods. *Int J Remote Sens* 31:1175–1192.
492 <https://doi.org/10.1080/01431160903380649>

493 Næsset E (2002) Predicting forest stand characteristics with airborne scanning laser using a practical
494 two-stage procedure and field data. *Remote Sens Environ* 80:88–99.
495 [https://doi.org/10.1016/S0034-4257\(01\)00290-5](https://doi.org/10.1016/S0034-4257(01)00290-5)

496 Næsset E, Bjercknes K-O (2001) Estimating tree heights and number of stems in young forest stands
497 using airborne laser scanner data. *Remote Sens Environ* 78:328–340. [https://doi.org/DOI:
498 10.1016/S0034-4257\(01\)00228-0](https://doi.org/DOI:10.1016/S0034-4257(01)00228-0)

499 NGI (2022) Snøskredulykker med død. In: *Norwegian Geotech. Inst.*
500 [https://www.ngi.no/Tjenester/Fagekspertise/Snoeskred/snoskred.no2/Snoeskredulykker-med-
501 doed](https://www.ngi.no/Tjenester/Fagekspertise/Snoeskred/snoskred.no2/Snoeskredulykker-med-dod)

502 Pinheiro J, Bates D, DebRoy S, et al (2020) nlme: Linear and Nonlinear Mixed Effects Models

503 R Core Team (2020) R: A language and environment for statistical computing.

504 Rätty J, Astrup R, Breidenbach J (2021) Prediction and model-assisted estimation of diameter
505 distributions using Norwegian national forest inventory and airborne laser scanning data. *Can J*
506 *For Res* 51:1521–1533. <https://doi.org/10.1139/cjfr-2020-0440>

507 Schmuldlach G, Köhler J (2016) Automated avalanche risk rating of backcountry ski routes. In:
508 *International Snow Science Workshop Proceedings. Breckenridge, Colorado, USA, pp 450–456*

509 Sharp AEA (2018) EVALUATING THE EXPOSURE OF HELISKIING SKI GUIDES TO AVALANCHE TERRAIN
510 USING A FUZZY LOGIC AVALANCHE SUSCEPTIBILITY MODEL. University of Leeds, School of
511 Geography

512 Statham G, McMahon B, Tomm I (2006) The avalanche terrain exposure scale. In: *Proceedings of the*
513 *International Snow Science Workshop. Telluride, CO, USA, pp 491–497*

514 Tarboton DG (2004) Terrain analysis using digital elevation models (TAUDEM)

515 Teich M, Bartelt P, Grêt-Regamey A, Bebi P (2012) Snow Avalanches in Forested Terrain: Influence of
516 Forest Parameters, Topography, and Avalanche Characteristics on Runout Distance. *Artic,*
517 *Antarct Alp Res* 44:509–519. <https://doi.org/10.1657/1938-4246-44.4.509>

518 Teich M, Fischer J-T, Feistl T, et al (2014) Computational snow avalanche simulation in forested
519 terrain. *Nat Hazards Earth Syst Sci* 14:2233–2248. <https://doi.org/10.5194/nhess-14-2233-2014>

520 Tompalski P, White JC, Coops NC, Wulder MA (2019) Quantifying the contribution of spectral metrics
521 derived from digital aerial photogrammetry to area-based models of forest inventory attributes.
522 *Remote Sens Environ* 234:111434. <https://doi.org/10.1016/J.RSE.2019.111434>

- 523 Varsom (2022) Dødsfall og skader fra snøskred og på islagte vann. <https://www.varsom.no/ulykker/>
- 524 Veitinger J, Purves RS, Sovilla B (2016) Potential slab avalanche release area identification from
525 estimated winter terrain: a multi-scale, fuzzy logic approach. *Nat Hazards Earth Syst Sci*
526 16:2211–2225. <https://doi.org/10.5194/nhess-16-2211-2016>
- 527 Venables WN, Ripley BD (2002) *Modern Applied Statistics with S*, 4th edn. Springer, New York
- 528
- 529